

ac gate-induced Fano resonance and peak splitting of conductance in a quantum dot

Mou Yang and Shu-Shen Li*

State Key Laboratory for Superlattices and Microstructures, Institute of Semiconductors, Chinese Academy of Sciences, Beijing 100083, China

(Received 23 November 2003; revised manuscript received 23 February 2004; published 27 July 2004)

We have investigated the conductance of a quantum dot system suffering an anti-symmetric ac gate voltage which induces the transition between dot levels in the linear regime at zero temperature in the rotating wave approximation. Interesting Fano resonances appear on one side of the displaced resonant tunnelling peaks for the nonresonant case or the peak splitting for the resonant case. The line shape of conductance (vs Fermi energy) near each level of the quantum dot can be decomposed into two profiles: a Breit-Wigner peak and a Fano profile, or a Breit-Wigner peak and a dip in both cases.

DOI: 10.1103/PhysRevB.70.045318

PACS number(s): 73.40.Gk, 73.23.-b, 73.63.Kv

In recent years much attention has been drawn to the electron transport in quantum dots (QDs), in which the quantum coherence, Coulomb on-site repulsion and the discrete levels play the important role at low temperatures.¹ When there are levels in the energy window of the leads, electrons can go through the QD. One can tune the bias voltage or the gate voltage to modify the level number of the QD sandwiched by the chemical potentials of the leads, therefore the transport properties are altered. Many interesting physical phenomena arise from the system, such as Coulomb blockade,^{2,3} photon-assistant tunnelling,⁴ quantum pump,^{5,6} Kondo effect,⁷⁻⁹ Fano resonance,¹⁰ etc.

Fano resonance¹¹ is a very interesting phenomenon in electron transport physics. If an absorbed impurity, stub or any other structure producing localized levels exists in an electron wave guide or a quantum wire, Fano resonance takes place,¹²⁻¹⁴ which is caused by the interference between the propagating path and localized orbital. Recently, a few theoretical and experimental works of Fano resonance in QD have been made in the static case.^{10,15-17} Racec *et al.*¹⁶ found that the conductance of a QD can be decomposed into two parts: a resonant one described by a Fano profile with a complex asymmetry parameter and a noncoherent background. Xiong *et al.*¹⁵ investigated the resonant transmission of electrons through a multilevel QD in the Coulomb blockade regime and found that the quantum interference between the path through the resonant level and the paths via nonresonant levels results in the Fano peaks. Göres *et al.* have observed asymmetric Fano resonances in a single-electron transistor device.¹⁰ On the other hand, the electron tunnelling through different time-dependent mesoscopic structures has been discussed in many papers. Wagner pointed out the transmission quenching¹⁸ and Kim *et al.* reported the Fano resonance^{19,20} of one or two time-dependent quantum wells. Aguado *et al.*²¹ studied the resonant tunnelling of photon sidebands within the transfer Hamiltonian framework, using two different models with classic and quantum electromagnetic fields illuminating the quantum well structure, because experimental realization of time-dependent heterostructure with high frequency often resorts to the infrared electromagnetic field.²² Oosterkamp *et al.* observed the electron resonant tunnelling via photon sideband of the states in a QD in their experiment.²² Sun *et al.*²³ theoretically explained the result

of it based on the model proposed in Ref. 24, a widely adopted model (often called adiabatic model), in which all the levels of the QD and leads are all varied with time cosinoidally but no inter-level transition occurs. According to the Tien and Gordon theory,²⁵ each time-dependent level can be viewed as many sidebands with the weight $J_n^2(V/\hbar\omega)$ in the energy space, where $J_n(\dots)$ is the n th order Bessel function, and V is the fluctuation magnitude of the levels. Many recent works are based on this model which can give reasonable results as compared with recent experiments.^{4,22} It is possible that the adiabatic model breaks down if the gates of the QD are configured symmetrically and applied with an anti-symmetric time-dependent gate voltage as in Fig. 1. This configuration allows electrons to transit between levels in the QD. When the gate voltage frequency matches the level span of QD approximately (i.e., the resonant or small detune case), the transition takes place apparently and the transport properties will be affected dramatically.

In this paper we investigate the conductance through the QD depicted in Fig. 1 in the linear regime at zero temperature by only considering the two lowest levels using the rotating wave approximation (RWA). We find that the conductance in the case of nonresonance shows a Fano resonance beside each resonant tunnelling peak which is displaced slightly, and in the case of resonance it shows a dip at the resonant tunnelling peak center. When the width of the peak is small (compared with some parameters) it splits into two individual peaks with different or identical widths for the nonresonant or resonant case. The inter-level transition-

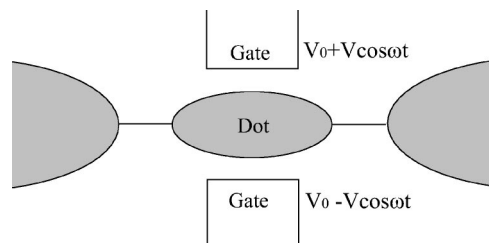


FIG. 1. Schematic configuration of the considered system. The QD experiences a dc gate voltage in addition to the anti-symmetric ac gate voltage, which allows electron transit between levels in the QD.

induced Fano resonance and peak splitting have not been investigated in the works mentioned in the previous paragraph. The Hamiltonian of the system is

$$H = \sum_{k,\alpha \in L/R} \epsilon_{k,\alpha} c_{k,\alpha}^\dagger c_{k,\alpha} + \sum_{k,\alpha,n} (V_{k,\alpha,n} c_{k,\alpha}^\dagger d_n + \text{h.c.}) + \sum_{n=1,2} \epsilon_n d_n^\dagger d_n + M \cos \omega t (d_1^\dagger d_2 + d_2^\dagger d_1), \quad (1)$$

where $c_{k,\alpha}^\dagger$ ($c_{k,\alpha}$) and d_n^\dagger (d_n) are the creation (annihilation) operators of electrons with momentum k in lead α and of electrons at level n in the dot. M is a parameter introduced to interpret phenomenologically the inter-level coupling in the QD, which is proportional to $(V/d)\langle \phi_1 | \vec{r} | \phi_2 \rangle$, where V is the magnitude of the ac gate voltage and d is the distance between the two gates, \vec{r} is the position vector of the electron in QD and ϕ_n are electron orbital functions in QD. In the above equation we neglect the spin of and interaction between electrons in the dot, which leads to Coulomb oscillation^{2,3} and the famous Kondo effect⁷⁻⁹ below the Kondo temperature, but these important effects are not our interest in this Letter.

Using the Keldysh formalism and equation of motion method the time-dependent current from the left lead into the dot is²⁴

$$J_L(t) = -\frac{2e}{\hbar} \int_{-\infty}^t dt' \int \frac{d\epsilon}{2\pi} \text{Im Tr} \{ e^{i\epsilon(t-t')/\hbar} \mathbf{\Gamma}^L(\epsilon) \times [\mathbf{G}^<(t,t') + f_L(\epsilon) \mathbf{G}^r(t,t')] \}, \quad (2)$$

where the boldfaced letters represent 2×2 matrixes. $\mathbf{\Gamma}^L(\epsilon)$, $\mathbf{G}^{r/a}(t,t')$ and $\mathbf{G}^<(t,t')$ are the coupling matrix, the retarded/advanced and Keldysh Green's functions of the QD, whose matrix elements are defined as

$$\Gamma_{mn}^L(\epsilon) = 2\pi \sum_k V_{k,L,m}^* V_{k,L,n} \delta(\epsilon - \epsilon_{k,L}), \quad (3)$$

$$\mathbf{G}_{mn}^{r/a}(t,t') = \mp i \theta(\pm t \mp t') \langle \{ d_m(t), d_n^\dagger(t') \} \rangle, \quad (4)$$

$$\mathbf{G}_{mn}^<(t,t') = i \langle d_n^\dagger(t') d_m(t) \rangle. \quad (5)$$

The time average current is $\bar{J}_L = (1/T) \int_0^T J(t) dt$, where $T = 2\pi/\omega$ is the period. In this work we use an alternative method to obtain the average current. Integrating Eq. (3) over t , \bar{J} is obtained directly:

$$\bar{J}_L = \int_{-\infty}^{\infty} J_L dt = -\frac{2e}{\hbar} \int d\epsilon \text{Im Tr } \mathbf{\Gamma}(\epsilon) \times [\mathbf{G}^r(\epsilon, \epsilon) + f_L(\epsilon) \mathbf{G}^<(\epsilon, \epsilon)]. \quad (6)$$

The time average current through the right contact has the same form and is equal to \bar{J}_L . At the first sight, Eq. (6) cannot give a correct result because a nonzero constant as integrated over infinity cannot converge at any finite quantity. For example, $\int dt C e^{i\epsilon t} |_{\epsilon=0} = C \cdot 2\pi \delta(\epsilon-0) |_{\epsilon=0}$. Although if one gets rid of $2\pi \delta(\dots)$, it converges correctly. So one must omit $2\pi \delta(\dots)$ hidden in the Green's functions $\mathbf{G}^r(\epsilon, \epsilon)$ and $\mathbf{G}^<(\epsilon, \epsilon)$ to obtain the correct result. After some simple algebra and ignoring terms of the order $O(M^2/\Delta^2)$, the average

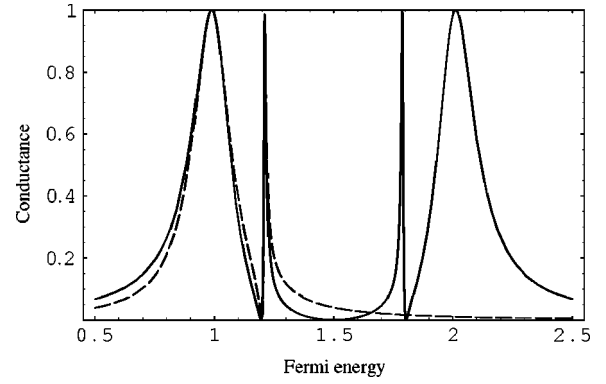


FIG. 2. Average conductance in units of e^2/h as a function of Fermi energy in arbitrary units with parameters $\epsilon_1=1$, $\epsilon_2=2$, $M=0.1$, $\gamma_1=\gamma_2=\gamma_{12}=\gamma_{21}=0.1$, and $\hbar\omega=0.8$ for both curves. The dashed curve is obtained using Eq. (10).

conductance at zero temperature in the linear regime can be obtained, which is just the Landauer type formula,

$$G = \frac{e^2}{h} \text{Tr} [\mathbf{\Gamma}^L(E_F) \mathbf{G}^a(E_F, E_F) \mathbf{\Gamma}^R(E_F) \mathbf{G}^r(E_F, E_F)]. \quad (7)$$

If the spin degeneracy is picked up, the conductance is doubled. To obtain an explicit result we assume the frequency is near the resonant point (i.e., $\hbar\omega/\Delta \approx 1$, where $\Delta = \epsilon_2 - \epsilon_1$) and M is small compared with the difference of the levels of the dot (i.e., $M/\Delta \ll 1$). This case allows us to employ the RWA. In the wide-band limit (i.e., $\mathbf{\Gamma}^{L/R}$ is independent of energy) and the symmetric case, we have

$$\mathbf{\Gamma}^L = \mathbf{\Gamma}^R = \begin{bmatrix} \gamma_1 & \gamma_{12} \\ \gamma_{21} & \gamma_2 \end{bmatrix}; \quad (8)$$

the retarded and advanced Green's functions with the same energy index are

$$\mathbf{G}^{r/a}(\epsilon, \epsilon) = \left[\begin{pmatrix} \frac{(\epsilon - \epsilon_1^+)(\epsilon - \epsilon_1^-)}{\epsilon - \epsilon_2 + \hbar\omega} & 0 \\ 0 & \frac{(\epsilon - \epsilon_2^+)(\epsilon - \epsilon_2^-)}{\epsilon - \epsilon_1 - \hbar\omega} \end{pmatrix} \pm \frac{i}{2} \mathbf{\Gamma} \right]^{-1}, \quad (9)$$

where $\mathbf{\Gamma} = \mathbf{\Gamma}^L + \mathbf{\Gamma}^R$, $\epsilon_1^\pm = \epsilon_1 - \delta/2 \pm \sqrt{\delta^2 + M^2}/2$ and $\epsilon_2^\pm = \epsilon_2 + \delta/2 \pm \sqrt{\delta^2 + M^2}/2$ are the dressed levels of the QD, where $\delta = \hbar\omega - (\epsilon_2 - \epsilon_1)$ is the detune. The derivation of the above equation will be given in the Appendix. Substitute Eq. (9) into Eq. (7) we get the average conductance. The solid curve in Fig. 2 is the average conductance vs Fermi energy with parameters $\gamma_1 = \gamma_2 = 0.1$, $\gamma_{12} = \gamma_{21} = \sqrt{\gamma_1 \gamma_2}$, $M = 0.1$, $\epsilon_1 = 1$, $\epsilon_2 = 2$ and $\hbar\omega = 0.8$. One can see there are two individual peaks near the energies ϵ_1 and ϵ_2 where the resonant tunnelling peaks are localized. Interestingly, there exist two sharp Fano resonances besides these peaks.

When the spacing between levels is much larger than the width of the individual peak, the conductance near each peak is little affected by the other, so when the Fermi energy is near ϵ_1 , we can reduce the conductance to a more simple form,

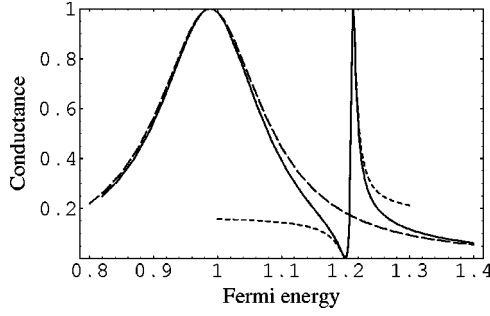


FIG. 3. Average conductance (solid line), Breit-Wigner and Fano profiles (long dashed and short dashed lines) in units of e^2/h as functions of Fermi energy with arbitrary units according to Eq. (10). All parameters are the same as in Fig. 2.

$$G = \frac{e^2}{h} \frac{\gamma_1^2 (E_F - \epsilon_2 + \hbar\omega)^2}{(E_F - \epsilon_1^+)^2 (E_F - \epsilon_1^-)^2 + \gamma_1^2 (E_F - \epsilon_2 + \hbar\omega)^2}. \quad (10)$$

In the following we will discuss in detail the features of the conductance curve based on the above equation in the case of $\delta < 0$. The dashed line in Fig. 2 is the curve obtained using Eq. (10) with the parameters just the same as for the solid line. One can see that the two lines coincide with each other near $E_F = \epsilon_1$. According to the above equation, when $E_F = \epsilon_1^\pm$ the conductance reaches its maximum and between the peaks it dives to zero when $E_F = \epsilon_2 - \hbar\omega$. The conductance profile near ϵ_1 can be decomposed into a Breit-Wigner and a Fano profile for the nonresonant case (see Fig. 3). The function of the Breit-Wigner profile is

$$G_{B-W} = \frac{e^2}{h} \frac{\gamma_1^2}{(\epsilon - \epsilon_1^-)^2 + \gamma_1^2}. \quad (11)$$

It is just the resonant tunnelling peak without ac gate voltage but the center of it is displaced to ϵ_1^- . The parameters of Fano resonance also can be worked out easily from Eq. (10), but we do not address them here for their complication and they will be demonstrated in the Appendix. The distance between the maxima of the two resonances is $\epsilon_1^+ - \epsilon_1^- = \sqrt{\delta^2 + M^2}$. When M goes down, the Breit-Wigner peak remains almost unchanged, but the Fano peak gets more sharp and vanishes if $M \rightarrow 0$. When δ reduces, the Fano peak moves towards the Breit-Wigner peak and becomes more dispersed. If δ goes to zero, a dip forms at $E_F = \epsilon_1$. The line shape near ϵ_1 can be decomposed into a Breit-Wigner peak (the long dashed line in Fig. 4) with the center at ϵ_1 and a dip (the short dashed line in Fig. 4) at the same energy ϵ_1 . The dip's line shape is described by

$$G_{Dip} = \frac{e^2}{h} \frac{(\epsilon - \epsilon_1)^2}{(\epsilon - \epsilon_1)^2 + (M^2/(4\gamma_1))^2}. \quad (12)$$

When γ_1 is smaller than the distance between the maxima localized at ϵ_1^\pm , these maxima evolve into two individual peaks with peak widths,

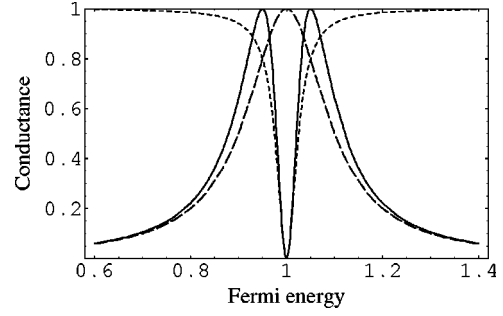


FIG. 4. Conductance (solid line), Breit-Wigner and dip line shapes (long dashed and short dashed lines) in units of e^2/h as functions of Fermi energy with arbitrary units. $\hbar\omega = 1$ and all other parameters are the same as in Fig. 2.

$$W_1^\pm = \gamma_1 \cdot \frac{\sqrt{1 + M^2/\delta^2} \mp 1}{\sqrt{1 + M^2/\delta^2}}. \quad (13)$$

One can see that the width of the peak at ϵ_1^- is wider than that at ϵ_1^+ and the latter vanishes if M goes to zero. When resonating, the widths of the two peaks become identical and are only half of the width of the resonant tunnelling peak without ac gate voltage.

When Fermi energy is in the vicinity of ϵ_2 , one can easily draw conclusions according to Fig. 2 and the analysis of the context. For the $\delta > 0$ case, the maxima of the Breit-Wigner peak and Fano peak in Fig. 3 are localized at ϵ_2^+ and ϵ_2^- instead of ϵ_1^- and ϵ_1^+ , which means the Fano peak is at the left side of the Breit-Wigner peak. In the asymmetric barrier case (i.e., $\Gamma^L \neq \Gamma^R$) the conductance is simply reduced but no new peak is introduced.

In fact, electron transport through ultra-small semiconductor QD is often dominated by Coulomb blockade effects. One extra electron added to the dot will constitute the charge energy U , which is inversely proportional to the total capacitance of the dot. It may be much larger than thermal fluctuation and Δ , just as in the experiment of Oosterkamp *et al.* (U is about 10 times Δ).²² Therefore, the large- U limit is valid and electrons can only tunnel sequentially through the dot. If we redefine ϵ_1 and ϵ_2 , respectively, as the energies of the top-most occupied level and the lowest empty level in the dot, when the Coulomb blockade is taken into account, the two sets of Breit-Wigner and Fano peaks in Fig. 2 localized approximately at ϵ_1 and $\epsilon_2 + U$ instead of ϵ_1 and ϵ_2 , but the line shapes of them are little affected. Adopting the parameters in Ref. 22, γ_1 and γ_2 are about 0.015 meV, Δ is 0.13 meV, and the corresponding frequency of the ac voltage is about 50 GHz. To induce a considerable transition between levels of the QD the ac voltage in that experiment should be magnified about $10^2 \sim 10^3$ times. The detailed description of the device has been in Ref. 22. This paper does not give an explanation to the result in it, since in our model the ac voltage is anti-symmetric.

Finally, let us examine all our conclusions following a heuristic argument. When an isolated QD is subjected to an anti-symmetric ac gate voltage, each level splits into two sublevels of which the separation is much smaller than that of levels. Therefore, near each level there are two resonant

maxima. The widened sublevels (due to the coupling to the leads) overlap each other severely, which leads to the interference between the two sublevels through which electrons penetrate the QD, so interference effects are observed such as Fano resonance and dip. Of course, more detailed features should rely on the calculations as in this paper.

In summary we have investigated the time-average conductance of QD with anti-symmetric gate voltage configuration in linear regime at zero temperature using RWA. We have observed a Fano resonance accompanying the displaced resonant tunnelling peak in the nonresonant case and the splitting of the resonant tunnelling peak in the resonant case. In the case that the width of the resonant tunnelling peak is small enough, it splits into two individual peaks which are different from each other in the nonresonant case and are identical in the resonant case.

ACKNOWLEDGMENTS

This work was supported by the National Natural Science Foundation of China and the special funds for Major State Basic Research Project No. G2001CB309500 of China.

APPENDIX A: GREEN'S FUNCTION OF THE QD

The Green's function in energy space of an isolated QD is

$$\begin{aligned} \mathbf{G}_0(\epsilon, \epsilon') &= \begin{bmatrix} \frac{2\pi\delta(\epsilon - \epsilon')(\epsilon - \epsilon_2 + \hbar\omega)}{(\epsilon - \epsilon_1^+)(\epsilon - \epsilon_1^-)} & \frac{2\pi\delta(\epsilon - \epsilon' + \hbar\omega)M/2}{(\epsilon - \epsilon_1^+)(\epsilon - \epsilon_1^-)} \\ \frac{2\pi\delta(\epsilon - \epsilon' - \hbar\omega)M/2}{(\epsilon - \epsilon_2^+)(\epsilon - \epsilon_2^-)} & \frac{2\pi\delta(\epsilon - \epsilon')(\epsilon - \epsilon_1 - \hbar\omega)}{(\epsilon - \epsilon_2^+)(\epsilon - \epsilon_2^-)} \end{bmatrix} \\ &= \mathbf{g}_0 + \mathbf{g}', \end{aligned} \quad (\text{A1})$$

where \mathbf{g}_0 and \mathbf{g}' are the diagonal and anti-diagonal parts of \mathbf{G}_0 . The infinitesimal in Green's function is ignored because the self-energy will bring a finite imaginary part. The total retarded (advanced) Green's function of the QD can be derived from Dyson's equation,

$$\begin{aligned} \mathbf{G}^{r/a} &= \mathbf{G}_0 + \mathbf{G}_0 \Sigma^{r/a} \mathbf{G}_0 + \dots \\ &= [(\mathbf{g}_0 + \mathbf{g}_0 \Sigma^{r/a} \mathbf{g}_0 + \dots) + O(M^2/\Delta^2)]_{\epsilon=\epsilon'} \\ &\quad + [O(M/\Delta)]_{\epsilon \neq \epsilon'}. \end{aligned} \quad (\text{A2})$$

Here $\Sigma^{r/a} = \mp i(\Gamma^L + \Gamma^R)/2$ is the retarded (advanced) self-energy. The physical origin of $[O(M/\Delta)]_{\epsilon \neq \epsilon'}$ and $[O(M^2/\Delta^2)]_{\epsilon=\epsilon'}$ is the photon-assistant transition and the combination of it and the effective coupling between two levels of the QD. Because they are much smaller than the term in the curved bracket they are omitted, which produces divarication of the order $O(M^2/\Delta^2)$ in the conductance. So the Green's function with the same energy index is

$$\mathbf{G}^{r/a}(\epsilon, \epsilon) = (\mathbf{g}_0^{-1} - \Sigma^{r/a})^{-1}. \quad (\text{A3})$$

Getting rid of $2\pi\delta(\epsilon, \epsilon')$ in the above equation, we obtain Eq. (9) in the text.

APPENDIX B: PARAMETERS OF FANO RESONANCE

The asymmetric Fano function¹¹ is described by

$$G_{\text{Fano}} = \frac{e^2}{h} \frac{A[m(\epsilon - t) + q]^2}{m^2(\epsilon - t)^2 + 1}, \quad (\text{B1})$$

where A is a normalization constant, t is the center of Fano line shape, m is the magnification coefficient and q is the Fano factor. Expanding the numerator and denominator in Eq. (10) around t and setting the coefficient of the first-order expansion of denominator to be zero, we obtain the Fano resonance center,

$$t = \epsilon_1^+ - \frac{\alpha \gamma_1^2}{\delta^2 + M^2 + \gamma_1^2}, \quad (\text{B2})$$

where $\alpha = \delta/2 + \sqrt{\delta^2 + M^2}/2$. Substituting Eq. (B2) into Eq. (10), one can work out all the parameters in Eq. (B1),

$$q = \frac{\sqrt{\delta^2 + M^2}}{\gamma_1^2}, \quad (\text{B3})$$

$$m = \frac{\delta^2 + M^2 + \gamma_1^2}{\alpha \gamma_1 \sqrt{\delta^2 + M^2}}, \quad (\text{B4})$$

$$A = \frac{\gamma_1^2}{\delta^2 + M^2 + \gamma_1^2}. \quad (\text{B5})$$

The line shape of Eq. (B1) is just the short-dashed line in Fig. 3.

*Corresponding author. Electronic address: sslee@red.semi.ac.cn

¹L. P. Kouwenhoven, C. M. Marcus, P. L. Mceuen, S. Tarucha, R. M. Westervelt, and N. S. Wingreen, *Electron Transport in Quantum Dots*, edited by J. P. Bird (Kluwer Academic, Dordrecht, 2003).

²Y. Meir, N. S. Wingreen, and P. A. Lee, Phys. Rev. Lett. **66**, 3048 (1991).

³Y. Nagamune, H. Sakaki, L. P. Kouwenhoven, L. C. Mur, C. J. P. M. Harmans, J. Motohisa, and H. Noge, Appl. Phys. Lett. **64**, 2379 (1994).

⁴Q. F. Sun, J. Wang, and T. H. Lin, Phys. Rev. B **61**, 12 643 (2000).

⁵Q. F. Sun, H. Guo, and J. Wang, Phys. Rev. Lett. **90**, 258301 (2003).

⁶E. R. Mucciolo, C. Chamon, and C. M. Marcus, Phys. Rev. Lett. **89**, 146802 (2002).

⁷T. K. Ng and P. A. Lee, Phys. Rev. Lett. **61**, 1768 (1988).

⁸Y. Ji, M. Heiblum, and H. Shtrikman, Phys. Rev. Lett. **88**, 076601 (2002).

⁹J. Martinek, Y. Utsumi, H. Imamura, J. Barnaś, S. Maekawa, J.

- König, and G. Schön, *Phys. Rev. Lett.* **91**, 127203 (2003).
- ¹⁰J. Göres, D. Goldhaber-Gordon, S. Heemeyer, M. A. Kastner, H. Shtrikman, D. Mahalu, and U. Meirav, *Phys. Rev. B* **62**, 2188 (2000).
- ¹¹U. Fano, *Phys. Rev. Lett.* **124**, 1866 (1961).
- ¹²S. A. Gurvitz and Y. B. Levinson, *Phys. Rev. B* **47**, 10 578 (1993).
- ¹³E. Tekman and P. F. Bagwell, *Phys. Rev. B* **48**, 2553 (1993).
- ¹⁴O. Olendski and L. Mikhailovska, *Phys. Rev. B* **67**, 035310 (2003).
- ¹⁵S. J. Xiong and Y. Yin, *Phys. Rev. B* **66**, 153315 (2002).
- ¹⁶E. R. Racec and U. Wulf, *Phys. Rev. B* **64**, 115318 (2001).
- ¹⁷M. L. Ladrón de Guevara, F. Claro, and P. A. Orellana, *Phys. Rev. B* **67**, 195335 (2003).
- ¹⁸M. Wagner, *Phys. Rev. B* **49**, 16 544 (1994).
- ¹⁹C. S. Kim and A. M. Satanin, *J. Phys.: Condens. Matter* **10**, 10587 (1998).
- ²⁰C. S. Kim and A. M. Satanin, *Physica E (Amsterdam)* **5**, 62 (1999).
- ²¹R. Aguado, J. Iñarrea, and G. Platero, *Phys. Rev. B* **53**, 10 030 (1996).
- ²²T. H. Oosterkamp, L. P. Kouwenhoven, A. E. A. Koolen, N. C. van der Vaart, and C. J. P. M. Harmans, *Phys. Rev. Lett.* **78**, 1536 (1997).
- ²³Q. F. Sun, J. Wang, and T. H. Lin, *Phys. Rev. B* **58**, 13 007 (1998).
- ²⁴N. S. Wingreen, A. P. Jauho, and Y. Meir, *Phys. Rev. B* **48**, 8487 (1993).
- ²⁵P. K. Tien and J. P. Gordon, *Phys. Rev.* **129**, 647 (1963).